Condensation of the plasma membrane at the site of T lymphocyte activation

Katharina Gaus,[1,2] Elena Chklovskaia,[3] Barbara Fazekas de St. Groth,[3] Wendy Jessup,[1,2] and Thomas Harder[4]

[1]Centre for Vascular Research at the School of Medical Sciences, University of New South Wales, Sydney 2052 NSW, Australia
[2]Department of Haematology, Prince of Wales Hospital, Sydney 2052 NSW, Australia
[3]Centenary Institute of Cancer Medicine and Cell Biology, University of Sydney, Sydney 2042 NSW, Australia
[4]Sir William Dunn School of Pathology, University of Oxford, Oxford OX1 3RE, England, UK

After activation, T lymphocytes restructure their cell surface to form membrane domains at T cell receptor (TCR)–signaling foci and immunological synapses (ISs). To address whether these rearrangements involve alteration in the structure of the plasma membrane bilayer, we used the fluorescent probe Laurdan to visualize its lipid order. We observed a condensation of the plasma membrane at TCR activation sites. The formation of ordered domains depends on the presence of the transmembrane protein linker for the activation of T cells and Src kinase activity. Moreover, these ordered domains are stabilized by the actin cytoskeleton. Membrane condensation occurs upon TCR stimulation alone but is prolonged by CD28 costimulation with TCR. In ISs, which are formed by conjugates of TCR transgenic T lymphocytes and cognate antigen-presenting cells, similar condensed membrane phases form first in central regions and later at the periphery of synapses. The formation of condensed membrane domains at T cell activation sites biophysically reflects membrane raft accumulation, which has potential implications for signaling at ISs.

Introduction

The activation of T lymphocytes is linked to the segregation of domains in the plasma membrane, which surrounds signaling machinery and the immunological synapse (IS; Dykstra et al., 2001; van der Merwe, 2002; Huppa and Davis, 2003; Harder, 2004). Within these domains, proteins and lipids assemble into complexes that mediate functions like T cell receptor (TCR) signal transduction and contact to antigen-presenting cells (APCs; Bunnell et al., 2002; Huppa and Davis, 2003). Plasma membrane–associated protein–lipid assemblies that transduce TCR signals have been analyzed morphologically and biochemically (Harder and Kuhn, 2000; Bunnell et al., 2002). After the triggering of TCR by immobilized anti-CD3 antibodies, multiple signaling proteins assemble in the plasma membrane in the vicinity of the TCR, coupling its activation to the induction of Ca^{2+} fluxes, activation of the Ras pathway, and actin nucleation (Dower et al., 2000; Bunnell et al., 2001; Wilde and Watson, 2001; Barda-Saad et al., 2005). Within these TCR-signaling domains, the transmembrane protein linker for activation of T cells (LAT) nucleates via phosphotyrosine-based docking motifs, complexes of cytoplasmic adaptor proteins such as Grb-2, GADs, and SLP-76, and enzymes like PLCγ (Zhang et al., 1998a; Tomlinson et al., 2000; Samelson, 2002).

Prominent membrane domains form at the IS, which is the contact zone of the T cell with its activating APC (van der Merwe, 2002). In most cases, the mature IS contains a central supramolecular activation cluster (cSMAC), which concentrates TCR and associated signaling proteins like LAT, Lck, and PKCτ (Freiberg et al., 2002). This cSMAC is surrounded by the peripheral SMAC, which enriches LFA-1 and talin (Monks et al., 1998). T cells that are deficient in WASp and Vav protein, which are both involved in nucleation and regulation of the actin cytoskeleton, show a defect in the formation of the IS after T lymphocyte activation (Krawczyk and Penninger, 2001; Villalba et al., 2002). Moreover, disruption of the actin cytoskeleton by cytochalasin D treatment blocks the formation of stable TCR assemblies and SMACs, further emphasizing its critical importance for the formation of the IS (Bunnell et al., 2001; Orange et al., 2003).

Correspondence to Katharina Gaus: k.gaus@unsw.edu.au; or Thomas Harder: thomas.harder@pathology.oxford.ac.uk

Abbreviations used in this paper: 3D, three dimensional; APC, antigen-presenting cell; cSMAC, central SMAC; DC, dendritic cell; DRM, detergent-resistant membrane; FRET, fluorescence resonance energy transfer; GP, generalized polarization; GPI, glycosylphosphatidyl-inositol; IS, immunological synapse; LAT, linker for activation of T cells; l_d, liquid disordered; l_o, liquid ordered; mβCD, methyl-β-cyclodextrin; MHC, major histocompatibility complex; PBL, peripheral blood lymphocyte; SMAC, supramolecular activation cluster; TCR, T cell receptor; TfR, transferrin receptor; TLA, TCR LAT–signaling assembly; WT, wild type.

The Journal of Cell Biology, Vol. 171, No. 1, October 10, 2005 121–131
http://www.jcb.org/cgi/doi/10.1083/jcb.200505047

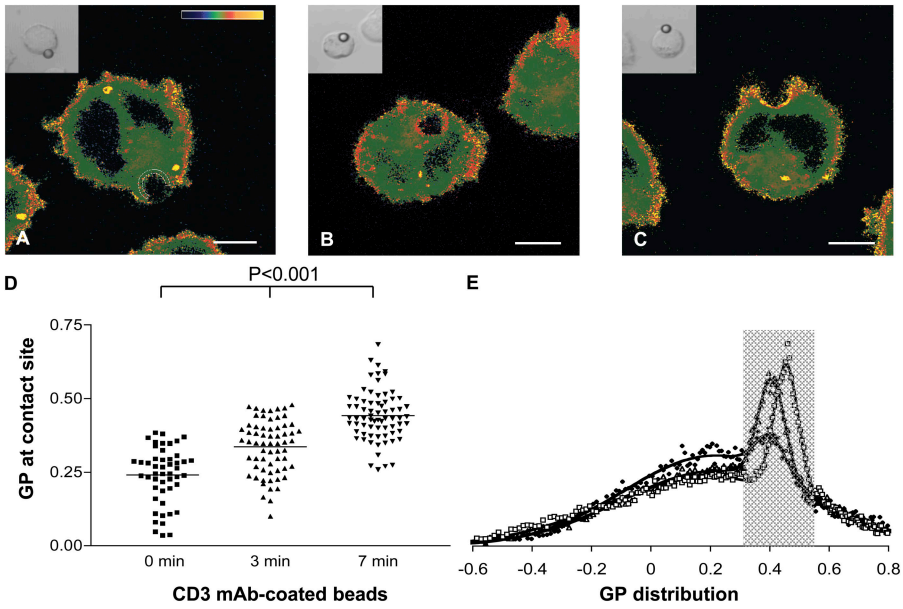

Figure 1. **Membrane condensation at the TCR activation site in Jurkat cells.** Laurdan-labeled JCaM2 cells expressing WT LAT were conjugated with α-CD3–coated polystyrene beads and incubated for 0 (A), 3 (B), and 7 (C) min at 37°C. Cells were adhered, fixed, and simultaneously imaged for the Laurdan intensity in two channels (400–460 nm and 470–530 nm). Intensity images were converted to GP images as described in Image analysis. (A–C) GP images were pseudocolored (see scale in A of GP −0.5–1), and insets show differential interference contrast (DIC) images. Bars, 5 μm. (D) GP values at the bead–cell contact area were determined as outlined by the white dashed line in A. Means (indicated by horizontal lines) and SDs are given in Table I. All datasets are significantly different to each other ($P < 0.001$). (E) GP distribution of 0- (diamonds; $n = 17$), 3- (triangles; $n = 18$), and 7-min (squares; $n = 20$) incubations from one representative experiment. Distributions were fitted to two Gaussian populations (solid lines) with mean GP values at 0.215 and 0.402 (0 min), 0.228 and 0.406 (3 min), and 0.201 and 0.456 (7 min). The high GP population (shaded area) covered 6.6 (0 min), 17.7 (3 min), and 21.0% (7 min) of all Laurdan-stained pixels.

The properties and functional role of the plasma membrane in T cell activation are a subject of intense investigation. In particular, TCR signaling was proposed to take place in membrane domains called lipid rafts (Janes et al., 2000; Dykstra et al., 2003). Lipid rafts are viewed as cholesterol- and sphingolipid-rich domains that "float" in an environment of more fluid regions that are composed of glycerophospholipids (Simons and Ikonen, 1997; Simons and Toomre, 2000; Kusumi et al., 2004). Moreover, rafts are envisioned as liquid-ordered (l_o) membrane phases, whereas surrounding nonraft regions are in a liquid-disordered (l_d) phase (Brown and London, 2000). Proteins with appropriate lipid anchors and affinities, including many signaling molecules, glycosylphosphatidyl-inositol (GPI)–anchored proteins, and dually acylated proteins, preferentially partition into raft domains (Simons and Ikonen, 1997). These raft components were initially defined by their insolubility in detergent Triton X-100 (i.e., via their association with detergent-resistant membranes [DRMs]; Brown and London, 1998). Indeed, in native cellular membranes, fluorescence resonance energy transfer (FRET) measurements showed that GPI-anchored and myristoylated/palmitoylated raft markers are clustered in cholesterol-dependent domains, which most likely do not exceed a few to tens of nanometers in size (Varma and Mayor, 1998; Zacharias et al., 2002; Sharma et al., 2004).

The role of raft domains in TCR signaling is implicated by the tight association of several major elements of TCR signal transduction, such as Lck tyrosine kinase and transmembrane adaptors including LAT, with DRMs (Katagiri et al., 2001). Fluorescence microscopy of the generic raft marker ganglioside GM1, which is stained by cholera toxin, showed its accumulation at the T cell activation site (Viola et al., 1999). However, biochemical studies detected neither GM1 nor cholesterol enrichment in membranes that were enriched in activated TCR complexes (Harder and Kuhn, 2000), nor did fluorescence microscopical analysis show an increased concentration of the generic raft marker GPI-anchored GFP in TCR activation sites (Bunnell et al., 2002; Glebov and Nichols, 2004). Hence, it remains unclear whether TCR signaling occurs in raft membrane domains.

We studied the physical properties of the plasma membrane in the vicinity of activated TCR and in the IS by using the Laurdan membrane probe in conjunction with two-photon laser scanning microscopy. Laurdan's fluorescence emission spectrum changes depending on the condensation and order of its membrane environment. This change in Laurdan's spectral properties has been used to define ordered phases in artificial membranes (Bagatolli et al., 2003). It further was shown that this technique could be transferred to cells; for example, in macrophages or neutrophils, condensed membranes cover a significant proportion of the cell surface and are frequently associated with actin-rich membrane protrusions (Gaus et al., 2003; Kindzelskii et al., 2004). In this study, we describe condensation of the plasma membrane at the site of activation in T cell lines and primary T lymphocytes. The formation of condensed membrane domains was induced by TCR triggering, and condensed phases were stabilized by the actin membrane skeleton.

Results

Accumulations of raft markers ganglioside GM1, cholesterol, or GPI-GFP in TCR-signaling assemblies were not detected in several studies (Harder and Kuhn, 2000; Bunnell et al., 2002; Glebov and Nichols, 2004). Because cellular raft domains are viewed as l_o phases within l_d bilayers, we measured the order of the plasma membrane lipid bilayer at the site of T lymphocyte

Table I. **GP values at bead–cell or cell–cell contact sites**

JCaM2 cells	WT LAT	All Y-F LAT	JCaM2
α-CD3 mAb			
0 min	0.240 ± 0.095 (n = 50)		
3 min	0.336 ± 0.091 (n = 64)		
7 min	0.442 ± 0.085 (n = 71)[a,d,g,h,n]	0.345 ± 0.082 (n = 49)[b,f,l,o]	0.247 ± 0.097 (n = 43)[i]
TfR mAb			
7 min	0.227 ± 0.106 (n = 60)[a,k]	0.222 ± 0.111 (n = 63)[b,l]	0.233 ± 0.063 (n = 53)[m]
α-CD3 mAb			
PP2 (7 min)	0.289 ± 0.104 (n = 35)[c,d]	0.265 ± 0.056 (n = 30)[e,f]	0.265 ± 0.087 (n = 34)
PP3 (7 min)	0.419 ± 0.053 (n = 34)[c]	0.322 ± 0.056 (n = 30)[e]	0.242 ± 0.095 (n = 32)
4 mM mβCD			
α-CD3 mAb (7 min)	0.347 ± 0.069 (n = 41)[g]	0.365 ± 0.095 (n = 26)	0.249 ± 0.082 (n = 29)
TfR mAb (7 min)	0.237 ± 0.081 (n = 40)	0.215 ± 0.084 (n = 41)	0.196 ± 0.083 (n = 41)
10 mM mβCD			
α-CD3 mAb (7 min)	0.229 ± 0.112 (n = 61)[h]	0.194 ± 0.075 (n = 36)[i]	0.172 ± 0.095 (n = 37)[i]
TfR mAb (7 min)	0.139 ± 0.078 (n = 41)[k]	0.138 ± 0.096 (n = 44)[l]	0.136 ± 0.080 (n = 39)[m]
α-CD3 mAb (7 min)			
+ 3 min latrunculin	0.252 ± 0.102 (n = 58)[n]	0.248 ± 0.084 (n = 52)[o]	0.237 ± 0.135 (n = 43)
TfR mAb (7min)			
+ 3 min latrunculin	0.257 ± 0.076 (n = 38)	0.347 ± 0.072 (n = 32)	0.256 ± 0.092 (n = 37)
PBL	**CD3 mAb**	**CD3 + CD28 mAb**	**CD28 mAb**
0 min	0.219 ± 0.068 (n = 43)	0.194 ± 0.075 (n = 48)	0.190 ± 0.076 (n = 40)
7 min	0.413 ± 0.06 (n = 44)[a,b]	0.343 ± 0.060 (n = 44)[a,e]	0.272 ± 0.086 (n = 44)[b,e]
23 min	0.313 ± 0.074 (n = 46)[c,d]	0.354 ± 0.083 (n = 44)[c,f]	0.275 ± 0.089 (n = 46)[d,f]
60 min	0.296 ± 0.095 (n = 45)	0.312 ± 0.070 (n = 42)[g]	0.248 ± 0.097 (n = 42)[g]
Naive T cell: APC	**Without antigen**	**With antigen**	
0 min	0.205 ± 0.099 (n = 105)	0.227 ± 0.093 (n = 107)	
3 min	0.276 ± 0.109 (n = 95)[a]	0.370 ± 0.082 (n = 93)[a,d,e]	
7 min	0.241 ± 0.079 (n = 86)[b]	0.422 ± 0.071 (n = 83)[b]	
23 min	0.187 ± 0.083 (n = 103)[c]	0.300 ± 0.100 (n = 92)[c]	
7 min			
PP2		0.235 ± 0.114 (n = 51)[d]	
PP3		0.402 ± 0.061 (n = 50)	
+ 3 min latrunculin		0.206 ± 0.082 (n = 53)[e]	

Means ± SDs are given for JCaM2 cells, PBLs, and synapses between naive T cells and DCs. For comparisons between WT LAT, All Y-F LAT, and JCaM2 cells, see Figs. 2–4. Superscripts indicate pairs of GP means, which were significantly different with $P < 0.001$ in JCaM2 cells (a–o), PBLs (e–g), and in naive T cells (a–e) and with $P < 0.05$ in PBLs (a–d).

activation. To do so, we used the membrane dye Laurdan, which aligns parallel to the phospholipids (Bagatolli et al., 2003). Laurdan does not preferentially partition into either lipid phase but undergoes a shift in its peak emission wavelength from ~500 nm in fluid membranes to ~440 nm in condensed membranes. We simultaneously recorded the Laurdan fluorescence intensity in two channels: 400–460 nm (condensed membranes) and 470–530 nm (fluid membranes). By expressing a normalized ratio of the two emission regions as given by the generalized polarization (GP), Laurdan fluorescence provides a relative measure of lipid order in cell membranes. Therefore, GP values, which range from −1 (very fluid) to +1 (very condensed), measure membrane fluidity with l_d domains in the range of approximately −0.05–0.25 and measure l_o domains in a range of 0.25–0.55 (Gaus et al., 2003).

Condensation of the lipid bilayer at the site of TCR activation in Jurkat cells

To assess the degree of lipid condensation at TCR-signaling sites, T leukemic Jurkat–derived TCR signaling–competent JCaM2 cells expressing wild-type (WT) LAT were labeled with Laurdan (Gaus et al., 2003). The cells were conjugated to polystyrene beads that were coated with TR66 anti-CD3 mAb and were subsequently warmed to 37°C, leading to TCR activation at the bead–cell contact site (Harder and Kuhn, 2000). The bead–cell conjugates were imaged by two-photon laser scanning microscopy, and GP values were taken as described in Microscopy and in Cells and reagents (Gaus et al., 2003). After a 3- or 7-min incubation at 37°C, Laurdan fluorescence revealed a region of high GP at the area of the plasma membrane that was in contact with anti-CD3–coated beads in WT LAT JCaM2 cells (Fig. 1, A–C). This is indicative of membrane condensation at the bead–cell contact site. For quantification, we determined the mean GP at the region of membrane–bead contact (Fig. 1 A) for >50 images (Fig. 1 D). The contact zone was selected as the membrane area that was adjacent to the bead with a mean width across the plasma membrane of 0.48 ± 0.11 μm (~2.5-fold the spatial resolution of the microscope). Mean GP values increased from 0.240 ± 0.095 at 0 min to 0.336 ± 0.091 at 3 min and 0.442 ± 0.085 at 7 min (Table I), indicating that stimulation of the TCR causes significant membrane condensation at the activation site. Fig. 1 E shows the GP distribution of all GP values (i.e., of total membranes) as a normalized histogram of >12 cell cross sections from one experiment. As described previously in macrophages (Gaus et al., 2003), a condensed membrane population with high mean GP

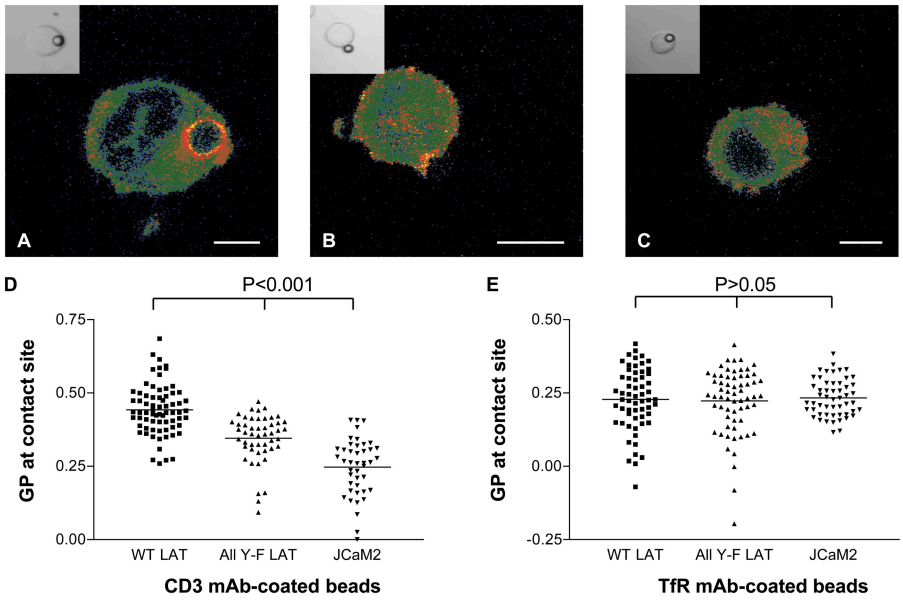

Figure 2. **Effect of LAT on membrane structure at TCR activation sites.** Laurdan-labeled JCaM2 cells expressing WT LAT (A), mutant All Y-F LAT (B), or the parent cell line without LAT (C) were conjugated with α-CD3–coated (A–D) or TfR-coated beads (E) and were incubated for 7 min at 37°C. Laurdan fluorescence was imaged and converted as described in Image analysis; GP images were pseudocolored as indicated in Fig. 1. Bars, 5 μm. Insets in A–C show DIC images. (D and E) GP values at the bead–cell contact sites were determined for individual images (Fig. 1 A). Means (indicated by horizontal lines) and SDs for are given in Table I. $P < 0.001$ for all comparisons within D, and $P > 0.05$ for comparison within E.

can be discriminated in these histograms (Fig. 1 E, shaded area). Importantly, the proportion of these condensed membranes as a percentage of total membranes significantly increased from 6.6 to 21.0% upon stimulation (7 min) of the Jurkat cells with anti-CD3 beads. Such changes in GP distribution were not observed when cells were conjugated to beads that were coated with antitransferrin receptor (TfR) mAb (high GP membranes as percentage of total membranes: 9.5% at 0 min, 9.0% at 3 min, and 10.7% at 7 min), which do not stimulate TCR-mediated signaling events (Harder and Kuhn, 2000). As the TCR activation site (Fig. 1 A, highlighted area) represents 7–13% of the surface area of the cell cross sections, membrane condensation at the anti-CD3 bead contact site accounts for the majority of the TCR triggering–induced membrane condensation that is seen in Fig. 1 E, with non-TCR sites contributing ~1–2% at 3 min and 4–5% at 7 min. The membrane condensation that is induced by TCR activation may be interpreted either as a de novo condensation of the lipid bilayer or as a coalescence of small preexisting rafts below the resolution of the microscope (<183 nm) at the bead–cell contact zone. Although we cannot distinguish between large continuous domains or clustered small ones, these experiments showed that condensed raftlike lipid domains, which are detectable by light microscopy, accumulate at the site of TCR activation by anti-CD3–coated beads.

Formation of ordered lipid phases in TCR-signaling domains depends on the transmembrane adaptor LAT and Src family kinase activity

The DRM-associated transmembrane adaptor LAT is a key nucleator of the TCR-signaling machinery (Zhang et al., 1998b). LAT with mutated tyrosine-based docking sites for cytoplasmic signaling proteins (All Y-F LAT) is incapable of transducing TCR signals (Lin and Weiss, 2001) and exhibits diminished accumulation at the site of TCR activation (Hartgroves et al., 2003). To test whether LAT is required for the formation of condensed, raftlike lipid membranes at the site of TCR activation, we used the JCaM2 Jurkat–derived cell line, which lacks LAT expression and, consequently, is incapable of transducing TCR signals (Lin and Weiss, 2001). We compared the GP values at the contact zone with anti-CD3–coated beads after 7 min of TCR stimulation in JCaM2 cells that were reconstituted with WT LAT (Figs. 1 and 2 A) or All Y-F LAT (Fig. 2 B) and in parental JCaM2 cells (Fig. 2 C). When compared with the WT LAT–expressing cells, JCaM2 cells expressing All Y-F LAT or the parental JCaM2 cells exhibited a significantly less ordering of lipids, as reflected by a reduced mean GP value at the TCR activation region (Fig. 2 D). Interestingly, JCaM2 All Y-F LAT cells (0.345 ± 0.082) exhibited an intermediate lipid order between JCaM2 WT LAT (0.442 ± 0.085) and parental JCaM2 cells (Table I; 0.247 ± 0.097), suggesting that properties of LAT that are independent of tyrosine-based docking sites are sufficient for plasma membrane condensation. Anti-CD3–coated beads induce the same membrane structure in parental LAT-null JCaM2 cells as non-TCR–stimulating TfR mAb–coated beads (Table I). Hence, LAT expression is critically important for the condensation of lipid membranes at the site of TCR activation. The role of different LAT protein motifs, such as different tyrosine-based docking regions, acylation sites, and possible cytoskeleton-interacting elements in this process, is not known and requires detailed investigation.

Next, we tested the role of Lck and Fyn activation in the condensation of TCR-signaling domains by using the inhibitor for Src-related kinases PP2 (Fig. 3 A) or the inactive control PP3 (Fig. 3 B). TCR-signaling domains in JCaM2 WT LAT cells that were treated with PP2 (0.289 ± 0.104) exhibited GP values that were as equally low as those of All Y-F LAT JCaM2 (0.265 ± 0.056) and the parental JCaM2 cell line (Table I; 0.265 ± 0.087). The noninhibitory PP2 analogue PP3 had no effects on the LAT-dependent increase in GP value at anti-CD3 bead contact sites (Fig. 3 B). These results show that Src kinase activity is required for membrane condensation in TCR-signaling domains.

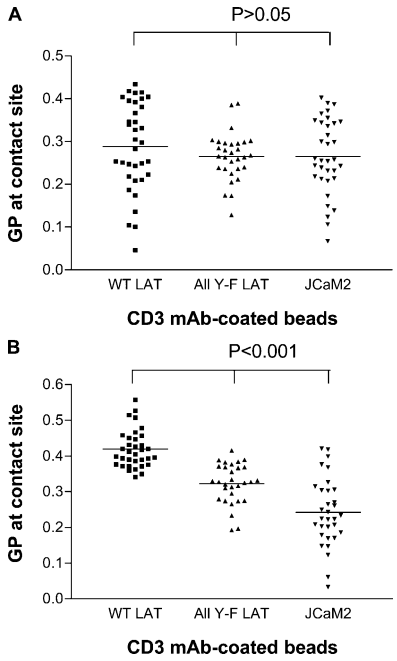

Figure 3. **Effect of Src kinase inhibitors on membrane structure at TCR activation sites.** Laurdan-labeled JCaM2 cells expressing WT LAT, mutant All Y-F LAT, or LAT-null parent cells were conjugated with α-CD3–coated beads and were incubated for 7 min at 37°C. Cells were preincubated for 1 h at 37°C with 10 μM PP2 (A) or the nonactive control PP3 (B). Inhibitors were also present during the incubation period after conjugation. Cells were imaged, and GP values of bead–cell contact sites were determined as described in Fig. 1. Means (indicated by horizontal lines) and SDs are given in Table I. For all comparisons within A and B, $P > 0.05$ and $P < 0.001$, respectively.

ingly, such treatment in Jurkat cells did not affect the earliest TCR-evoked tyrosine phosphorylation events and the formation of TCR LAT–signaling assemblies (TLAs; Harder and Kuhn, 2000). In this study, we tested whether cholesterol depletion affects the formation of ordered membrane phases. We used two previously characterized extraction conditions (Harder and Kuhn, 2000): preincubation with 4 mM mβCD for 40 min, which removed 42.6 ± 1.3% of cellular cholesterol, and preincubation with 10 mM for 25 min, which removed 55.6 ± 1.8% of cholesterol. Pretreatment with 4 mM mβCD partially impaired membrane condensation at the contact sites after 7 min of conjugation at 37°C with anti-CD3 mAb–coated beads in WT LAT–expressing JCaM2 cells ($P < 0.001$ compared with untreated control; Table I). However, it had no significant effect on CD3-conjugated All Y-F LAT JCaM2 ($P > 0.05$) or parent JCaM2 cells ($P > 0.05$) and had no effect on the membrane structure of any cell type when conjugated to anti-TfR–coated beads (Table I). Pretreatment with 10 mM mβCD significantly decreased ordered phases in conjugates of WT LAT JCaM2 ($P < 0.001$), All Y-F LAT JCaM2 ($P < 0.001$), and parent JCaM2 cells ($P < 0.001$) with anti-CD3–coated beads. Moreover, GP values at contact zones with anti-TfR–coated beads were also decreased by 10 mM mβCD pretreatment for all three cell types ($P < 0.001$; Table I). In conclusion, mβCD treatment completely impairs the formation of condensed membrane domains at TCR-signaling regions with 10 mM mβCD extraction, but the effects on lipid packing are not restricted to TCR activation sites. If extraction was performed with 4 mM mβCD, membrane condensation at the TCR activation site was reduced specifically but was not abolished.

Cholesterol extraction impairs membrane condensation at TCR activation sites

The formation of l_o phases depends on the presence of cholesterol (Sankaram and Thompson, 1991). Thus, it is believed that the integrity of cellular rafts requires cholesterol. Indeed, cholesterol depletion from thymocytes by methyl-β-cyclodextrin (mβCD) was shown to disrupt the association of most raft markers with DRM, including LAT and Lck (Kabouridis et al., 2000). Interest-

Condensation of TCR lipid domains is stabilized by the actin cytoskeleton

A role of LAT in the formation of actin-rich structures after TCR activation is well established (Bunnell et al., 2001; Barda-Saad et al., 2005). Filamentous actin accumulated at the contact zone between JCaM2 WT LAT cells with anti-CD3 beads (Fig. 4 B). We addressed the role of the actin cytoskeleton in the formation of ordered lipid domains at the bead–cell

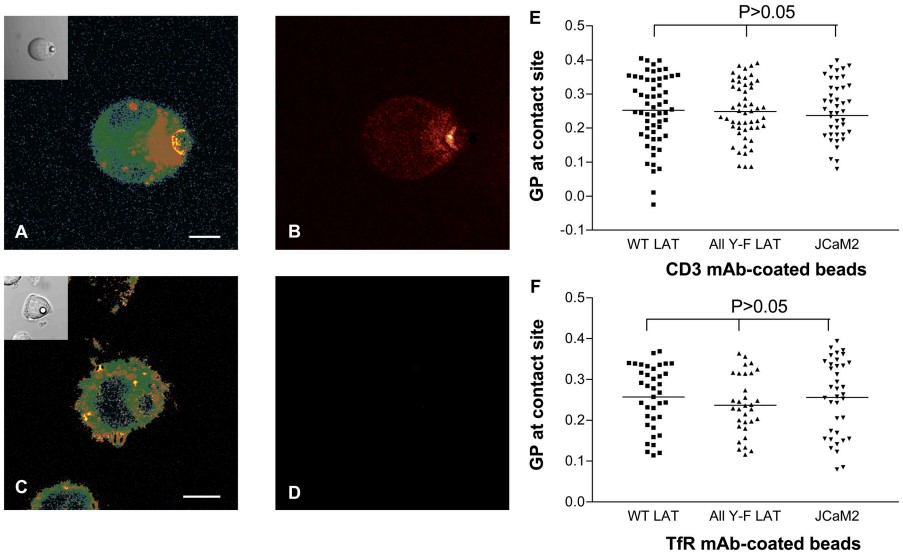

Figure 4. **Effect of actin depolymerization on membrane structure at the TCR activation site.** Laurdan-labeled JCaM2 cells expressing WT LAT, mutant All Y-F LAT, or LAT-null cells (JCaM2) were conjugated with α-CD3–coated (A–E) or TfR-coated (F) beads and were incubated for 7 min at 37°C (A and B) followed by the addition of 12.5 μM latrunculin B and incubation for a further 3 min at 37°C (C–E). (A and C) GP images were obtained and pseudocolored as described in Fig. 1. Insets show DIC images. (B and D) F-actin staining with phalloidin–Alexia 637. Note that no F-actin was detected in latrunculin B–treated cells (D). Bars, 5 μm. (E and F) GP values at contact sites between α-CD3–coated (E) or TfR-coated (F) beads and cells after latrunculin B treatment. Means (indicated by horizontal lines) and SDs are given in Table I. For all comparisons within E or F, $P > 0.05$. For all cell types, no statistically significant difference ($P > 0.05$) was found between means of α-CD3– and TfR-coated beads.

contact zone by using the fungal metabolite latrunculin B, which causes actin depolymerization. We stimulated JCaM2 cells with anti-CD3–coated beads for 7 min at 37°C. The conjugates were subsequently treated with 12.5 μM latrunculin B for a further 3 min at 37°C, leading to the loss of phalloidin staining (Fig. 4 D). GP values at the anti-CD3–coated bead-to-cell contact sites were significantly decreased for WT LAT–expressing cells ($P < 0.001$ compared with untreated controls; Table I) and for All Y-F LAT–expressing JCaM2 cells ($P < 0.001$) but not for parent JCaM2 cells ($P > 0.05$), therefore abolishing all differences between CD3- and TfR-conjugated cells (Fig. 4, E and F). Latrunculin B treatment had no effect on GP value at the site of TfR conjugation (Fig. 4 E). These experiments demonstrated that the maintenance of membrane condensation at TCR activation sites requires the continued integrity of the actin cytoskeleton.

Costimulation by CD28 prolongs membrane condensation at TCR activation sites

Full activation of primary resting T lymphocytes requires the engagement of costimulatory receptors in addition to the TCR and, most prominently, the engagement of CD28 with the B7 antigen receptor (Acuto and Michel, 2003). It was reported that TCR and CD28 engagement is required for GM1 polarization toward the site of T lymphocyte activation, which is interpreted as raft recruitment to the TCR activation site (Viola et al., 1999; Tavano et al., 2004). To test the role of CD28 costimulation in the formation of raftlike ordered membrane domains, we isolated resting peripheral blood lymphocytes (PBLs) from human donors and stimulated them with anti-CD3 (Fig. 5 A), anti-CD28 alone (Fig. 5 C), or anti-CD3/CD28-coated beads (Fig. 5 B). We followed the membrane structure at the contact site between 0 and 60 min after stimulation at 37°C. Conjugation with anti-CD3–coated beads showed a rapid condensation after 7 min (0.413 ± 0.06; Table I) followed by a significant decrease in lipid order (23 min; 0.313 ± 0.074). Stimulation with CD28 alone exhibited a lower initial membrane condensation than CD3 ligation, which remained stable for at least 60 min (0.248 ± 0.097). Costimulation with CD3 + CD28 also induced an initial increase of the mean GP value (7 min; 0.343 ± 0.060). Compared with CD3 stimulation alone, membrane condensation was sustained for longer (23 min; 0.354 ± 0.083). In conclusion, CD3 alone is sufficient for the initial formation of condensed membrane domains at the TCR activation site, yet costimulation with CD28 stabilizes condensed membrane structures for longer times.

Formation of ordered phases at the IS

The aforementioned experiments were performed with T leukemic cells and T lymphocytes that were stimulated with mAb-coated beads. To monitor the formation of ordered membrane phases at the IS and to verify our findings in a more physiological system, we used primary T cells that were isolated from lymph nodes of 5C.C7 TCR transgenic mice. As APCs, dendritic cells (DCs) were isolated from spleens of WT mice and were pulsed with cytochrome c. Alternatively, Jurkat

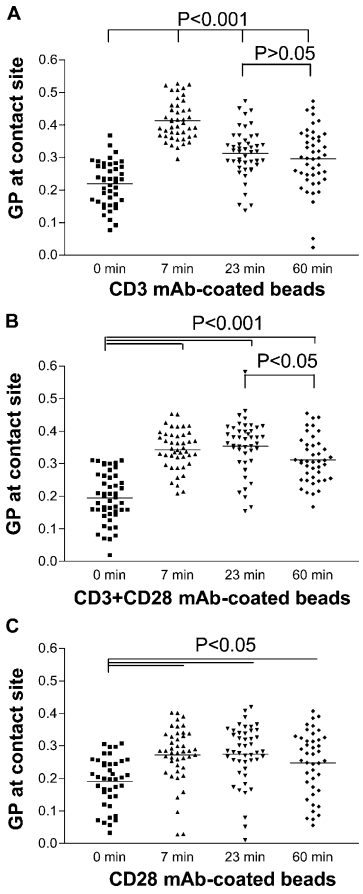

Figure 5. **Membrane structure at PBL activation sites.** Laurdan-labeled PBLs were conjugated with beads coated with α-CD3 mAb (A), a combination of α-CD3 and CD28 mAb (B), or CD28 mAb alone (C) and were incubated for 0–60 min at 37°C. Imaging and GP quantification at the contact site were performed as described for Fig. 1. (A) All datasets are significantly different to each other ($P < 0.001$) with the exception of 23 and 60 min, for which $P > 0.05$. (B) The mean of 0-min incubation is significantly different from 7, 23, and 60 min ($P < 0.001$), and differences between 23 and 60 min were also significant ($P < 0.05$); all other sets of data were not significantly different. (C) Only the means of 0 min is significantly different from 7, 23, and 60 min ($P < 0.05$). Means (indicated by horizontal lines) and SDs are given in Table I.

cells that were transfected with 5C.C7 to recognize cytochrome c (Jurkat 8.2) were used in conjunction with B cells from a cell line (CH27) as APCs. Conjugates were formed by pelleting both cell types together (10-s spin) followed by resuspension and incubation at 37°C for 0–23 min. Although only T cells were labeled with Laurdan, the dye rapidly distributed over both cells in the conjugates. Cell-tracking dye (CMRA) was loaded into APCs in order to discriminate between APCs and T cells in the conjugates.

We observed a significant increase of GP values at the contact zone after 3 min of incubation between T cells and APCs; both were in conjugates with (Table I; 0.370 ± 0.082) and without antigen (0.276 ± 0.109; $n = 95$; $P < 0.001$ ± antigen), but this was more intense and was sustained for longer in antigen-pulsed conjugates (Fig. 6). At 7 min, lipid order had decreased for cells that were conjugated without antigen (Fig. 6 C) but further increased (to 0.422 ± 0.071) for conjugates with antigen present (Fig. 6 G). At this time, in the presence of the antigen,

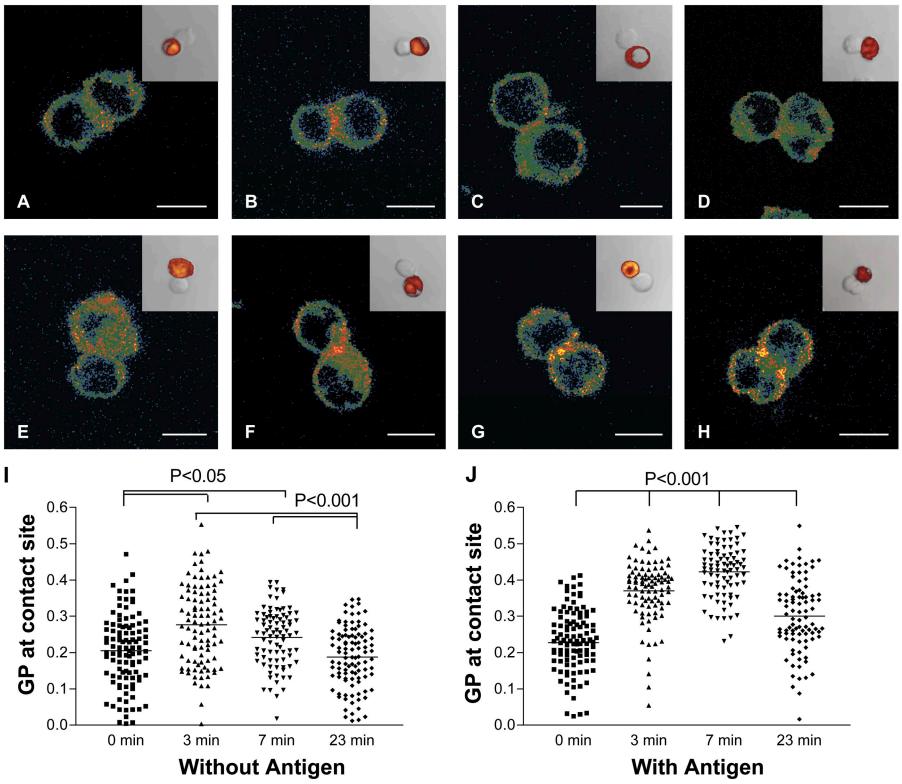

Figure 6. **Membrane structure at ISs.** (A–H) Laurdan-labeled naive T cells were conjugated to CMRA-labeled DCs for 0 (A and E), 3 (B and F), 7 (C and G), or 23 (D and H) min. Before conjugation, APCs were incubated in the absence (A–D and I) or presence (E–H and J) of 2 μM antigen cytochrome c. Cell couples were fixed and imaged as described for JCaM2 cells in Image analysis. Insets show the corresponding transmission image with the orange fluorescence image of CMRA overlaid to identify APCs. Bars, 5 μm. Imaging and pseudocoloring were performed as described in Fig. 1. (I and J). GP values measured over the entire contact area between primary T cell–APC couples without (I) and with (J) conjugation of APCs with antigen. Means (indicated by horizontal lines) and SDs are shown in Table I. (I) Differences were found between the means of 0 and 3 min or 7 min ($P < 0.05$) and the means of 23 and 3 min or 7 min ($P < 0.001$); other comparisons did not reveal significant differences. (J) All means are significantly different to each other ($P < 0.01$ or $P < 0.001$).

the condensed membrane domains were predominately localized at the central region of the IS (Fig. 6 G), which is in contrast to the 23-min time point in which ordered domains had moved away from the central area and associated more with peripheral areas of the synapses (Fig. 6 H). The mean GP value of synapses at 23 min decreased significantly (0.300 ± 0.100) compared with that after a 7-min incubation but remained above the mean without antigen present (0.187 ± 0.083; $P < 0.001$ ± antigen). For more spatial information, we constructed three-dimensional (3D) images and z-sectioned them at the IS, using conjugates of Jurkat 8.2 cells because they yielded a better resolution in z-direction (Fig. 7). As observed in the IS of transgenic T lymphocytes, these cells exhibited an increase of GP value if stimulated by antigen-pulsed APCs (Fig. 7, A and C). Like in primary T cells, this membrane condensation occurred initially at the contact zone to the APC and later moved to more peripheral sites (Fig. 7 C). These images show a reorganization of membrane condensation at the IS to peripheral regions.

Treatment with PP2, as performed for JCaM2 cells, decreased the lipid order of the synapse of antigen-containing conjugates of primary T cells after a 7-min incubation to 0.234 ± 0.114 ($P < 0.001$) compared with untreated controls (Table I), and no raftlike domains were identified in the central region of the synapses (not depicted). Treatment with PP3 had no effect ($P > 0.05$). Incubation of antigen-containing conjugates with latrunculin B reversed the formation of condensed membrane domains at the IS ($P < 0.001$). These experiments demonstrated that, in naïve T cells, raftlike domains are first formed at the central region of the IS by a Src kinase–dependent pathway and are stabilized by the underlying actin cytoskeleton. At later time points, condensed membrane domains are found at the periphery of synapses, suggesting an ongoing membrane remodelling and restructuring process.

Discussion

In this study, we monitored the structure of the T lymphocyte plasma membrane during activation by using the fluorescent dye Laurdan. If incorporated into a lipid membrane, Laurdan's

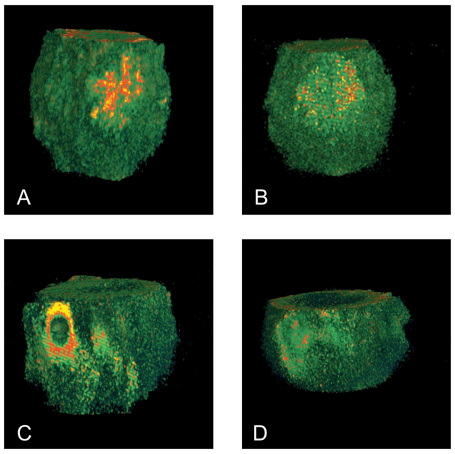

Figure 7. **3D reconstructed ISs.** Laurdan-labeled Jurkat 8.2 cells expressing C5.C7 to recognize cytochrome c were conjugated to CMRA-labeled B cells in the presence (A and C) or absence (B and D) of cytochrome c and were incubated for 7 (A and B) or 23 (C and D) min. Stacks of GP images of cell couples were 3D reconstructed and optically cut in the z-plane. Images in A–D show the z-plane of the synapse of the T cell; APCs are not visible. Imaging and pseudocoloring were performed as described in Fig. 1.

emission spectrum changes with the level of lipid ordering, allowing quantification of condensation and order of its bilayer environment. We used two-photon laser scanning microscopy of Laurdan fluorescence to show that the plasma membrane condenses at the regions of T cell activation. This membrane condensation requires the activity of Src-related kinases, the presence of LAT, and an intact actin cytoskeleton. Plasma membrane condensation was detected in JCaM2 Jurkat–derived T leukemic cells that were stimulated by beads coated with anti-CD3 antibody and beads in the IS that formed between TCR transgenic T lymphocytes and specific APCs.

Condensation of membrane domains indicates that ordered phases, which are, by definition, lipid rafts (Brown and London, 1998), accumulate or form in the T cell plasma membrane in the vicinity of TCR activation. It has been previously proposed that TCR signaling takes place in raft domains of the T cell plasma membrane (Dykstra et al., 2003). Several membrane proteins that are involved in early TCR signaling, like Src-related kinases Lck and Fyn and adaptor proteins like LAT, are associated with DRMs and, thus, are viewed as tightly raft-anchored proteins (Katagiri et al., 2001). Moreover, TCR components appear in DRMs after TCR activation (Montixi et al., 1998). A microscopic analysis of generic raft marker GM1 stained with cholera toxin showed accumulation at the activation region of T cells (Viola et al., 1999). This GM1 enrichment required ligation of the costimulatory molecule CD28 together with TCR. In contrast, biochemical analysis of immunoisolated TCR LAT signaling complexes from T leukemic Jurkat cells detected neither GM1 nor cholesterol enrichment (Harder and Kuhn, 2000). Moreover, fluorescence microscopy and FRET analysis of Jurkat cells showed no clustering of the generic raft marker GPI-anchored GFP in TCR activation sites (Bunnell et al., 2002; Glebov and Nichols, 2004). Because of this conflicting evidence and the remaining open questions about the relationship of DRMs and lipid rafts (Munro, 2003), the involvement of rafts in T cell activation has been a matter of discussion. We describe clustering of ordered domains in TCR activation domains, whereas generic chemical raft markers are not detectably accumulated. It will be necessary to determine the level of partitioning and anchoring of chemical raft markers in ordered membrane domains to elucidate this apparent discrepancy. Moreover, we find that extraction with mβCD results in a very significant reduction of the GP value at the anti-CD3 bead–T cell contact site, highlighting the importance of cholesterol in membrane condensation at TCR-signaling regions. This provides further support for the accumulation of ordered lipid phases, which have the biophysical hallmarks of rafts. The reduction of membrane order in the TCR-stimulated T cell line upon cholesterol extraction was not as strong as for cholesterol extraction in resting neutrophil cells (Kindzelskii et al., 2004), which is probably a result of differences in experimental conditions.

Two alternative processes can be envisaged to be responsible for the condensation of the plasma membrane at T cell activation sites. First, preexisting l_o domains may move to the cell pole that is engaged in T cell activation. This could involve passive diffusion of raft domains and raft constituents followed by their retention at TCR-activating regions or a directed active transport of raft components to these sites (Rodgers et al., 2005). Second, activation-induced membrane condensation may be a de novo formation of ordered phases driven by the localized anchoring of membrane proteins to actin filaments, thus introducing a diffusion barrier for lipids (Kusumi et al., 2004). Most likely, this involves the formation of multimolecular signaling complexes around LAT (Bunnell et al., 2001). Together, these processes may explain the observed sensitivity of membrane condensation to LAT deficiency and actin destabilization. Similar processes may be responsible for raft coalescence (Harder and Simons, 1999) and for the formation of high GP domains (Gaus et al., 2003) that are induced by the cross-linking of membrane proteins.

Our histograms of ordered membrane occurrence in activated T cells indicate such de novo membrane condensation. However, it has to be taken into account that condensed raftlike domains may exist in nonstimulated T cells in sizes below the resolution of a light microscope (182 nm in diameter). Upon concentration at the sites of T cell activation, preexisting rafts would achieve detection by light microscopy, giving rise to a distinct peak in the histograms. In summary, an important issue for future studies will be whether preexisting condensed phases move to sites of T cell activation or whether the ordered membrane phases form de novo.

In resting cells, small raft domains are likely to control the transient interaction between membrane proteins. Several studies addressed the distribution of generic raft markers in native cellular plasma membranes by FRET measurements (Zacharias et al., 2002; Sharma et al., 2004). These experiments showed the existence of nanometer-sized clusters around GPI-anchored proteins in the outer leaflet of the plasma membrane or myristoylated/palmitoylated proteins in the inner leaflet of the plasma membrane. The small size of all of these clusters is likely to reflect rapid exchange and transient encounters between two raft-associated proteins, whereas encounters with nonraft membrane proteins are less likely. Such raft-controlled interactions are exemplified in the binding of raft-anchored Lck to CD8 dimers. The CD8α subunit of the CD8 dimer provides an intracellular Lck-binding site and extracellular major histocompatibility complex (MHC) class I docking. Thus, the CD8β subunit, by providing a palmitoylation raft-targeting site (Arcaro et al., 2000), endows the CD8αβ dimer with a more efficient MHC class I coreceptor function as compared with the CD8αα dimer (Arcaro et al., 2001). This may be explained by raft-controlled interactions of Lck kinase; raftlike phases around CD8αβ are miscible with the Lck environment, whereas CD8αα outside of rafts interacts with raft-anchored Lck less efficiently.

We observed larger and more stable ordered lipid domains at sites of T cell activation. Lipids alone form ordered phases in artificial membranes, whereas (besides the lipids) proteins mediate the formation and stabilization of condensed domains in cell membranes. The formation of such large-scale raft domains may be partially driven by the assembly of TLAs: for example, by anchoring palmitoylated membrane protein LAT in the environment of activated TCR (Harder and Kuhn,

2000; Bunnell et al., 2002). TLA formation is mediated by the tyrosine phosphorylation of LAT and the subsequent binding of SH2 domain–containing proteins to cognate phosphotyrosine motifs (Hartgroves et al., 2003). By tracking single LAT molecules, it was recently shown that proteins also mediate recruitment and anchorage of LAT into plasma membrane domains, which cluster CD2 (Douglass and Vale, 2005). Like TLAs, these CD2 clusters did not detectably anchor generic raft markers (Harder and Kuhn, 2000; Douglass and Vale, 2005). Taking TCR LAT assemblies as precedence, it seems probable that CD2-LAT domains contain ordered membranes and, therefore, have biophysical raft properties.

Inhibition of tyrosine kinase activity blocks membrane condensation at TCR activation sites, and we conclude that TCR signaling precedes membrane condensation. The binding of cytoplasmic adaptors and enzymes to phosphorylated LAT-signaling assemblies is cooperative (i.e., the association of proteins like Grb2 and PLCγ further promotes TLA assembly). It is likely that such cooperation involves networks of LAT and signaling proteins. Accordingly, condensed domains are likely to play an important role in the assembly of TLAs. In line with this hypothesis, the raft-deficient LAT variant lacking palmitoylation sites is incapable of forming TLAs and transducing TCR signals (Zhang et al., 1998b; Harder and Kuhn, 2000). Moreover, the formation of stable, large raft domains by cholera toxin-GM1 cross-linking creates tyrosine-phosphate–containing hotspots, possibly by generating a kinase-favorable environment and the exclusion of phosphatases like CD45 (Harder and Simons, 1999).

Laurdan staining has revealed condensed lipid domains in macrophage plasma membranes that are connected to actin-rich membrane protrusions (Gaus et al., 2003). Together with the sensitivity of membrane condensation to actin depolymerization that is demonstrated in this study, these observations indicate a connection between cortical cytoskeletal actin and large-scale ordered membrane domains. It is possible that by recruiting activated actin regulatory small GTPases like Rac1 to signaling complexes in condensed membrane phases (del Pozo et al., 2004), these lipid domains help generate actin-rich structures. This would create a positive feedback loop between the actin filaments and the ordered lipid bilayer in as much as actin filaments support the formation of condensed lipid domains, whereas, vice versa, condensed membranes promote the formation of the actin cytoskeleton.

The immune synapse requires the actin cytoskeleton and actin-regulating proteins Vav and WASp to prime T cells for activation (Bunnell et al., 2001; Villalba et al., 2001). Thus, the interplay between membrane condensation and actin organization could provide a "switch" to turn on T cell function and immunity. Interestingly, in the IS, condensed membranes are first formed in central regions and are then rearranged to more peripheral sites. Thus, the first signaling events in response to TCR engagement, like Lck tyrosine kinase activation, ZAP-70 recruitment, LAT phosphorylation, and TLA formation, coincide with membrane condensation in the central region of the IS. The reorganization of ordered membranes in the IS to peripheral sites may be linked to the reorganization of the cytoskeleton, which is reflected by talin rearrangement from cSMACs to peripheral SMACs (Monks et al., 1998; Freiberg et al., 2002).

The lipid bilayer of the plasma membrane serves as a matrix for early signal transduction, and the principles found in this study may apply to other systems involving surface receptors. Rafts are likely to serve as a scaffold for the generation of multimolecular signaling machineries. An understanding of the functional consequences of membrane condensation requires further studies to elucidate the nature of the interplay between the newly formed condensed domains and membrane-associated signaling proteins in T cells and other signaling systems. Furthermore, reorganization of these domains, possibly in connection with cytoskeletal restructuring, could critically determine the functional outcomes of signaling cascades and requires an understanding of the molecular mechanisms of the cross talk between the actin cytoskeleton and condensed plasma membrane domains.

Materials and methods

Mice

Naive T cells were purified from mice transgenic for the α and β chains of 5C.C7 TCR that recognize the COOH-terminal epitope of moth cytochrome c ($MCC_{87–103}$) in association with MHC class II IE^k (Fazekas de St. Groth et al., 1993; Seder et al., 1992). The transgenic line was maintained on a rag2−/− B10.BR ($H\text{-}2^k$) background. DCs were obtained from WT B10.BR mice. All mice were bred and housed under specific pathogen-free conditions at the Centenary Institute Animal Facility. Approval for animal experimentation was obtained from the Institutional Ethics Committee at the University of Sydney.

Cells and reagents

Jurkat-derivative JCaM2 cells, Jurkat 8.2 cells, and the B cell line CH27 were cultured in RPMI containing 10% (vol/vol) FBS at 37°C in 5% CO_2. JCaM2 clones with a stable expression of WT LAT or All Y-F LAT (obtained from J. Lin and A. Weiss, University of California, San Francisco, San Francisco, CA; Lin and Weiss, 2001; Hartgroves et al., 2003) and Jurkat 8.2–expressing 5C.C7 (Matthias et al., 2002) were described previously. PBLs were isolated from a peripheral blood mononuclear cell suspension by negative depletion, removing CD19-, CD14-, and CD16-positive cells (MACS separation; Miltenyi Biotec). Peripheral blood mononuclear cells were isolated by Ficoll-Plaque (GE Healthcare) density gradient centrifugation from EDTA-treated human blood from healthy volunteers. PBL purity was >93%. Naive T cells were purified from peripheral lymph nodes of TCR transgenic mice by negative selection using magnetic depletion of CD19 (clone 1D3), Gr-1, and Mac-1–positive cells (autoMACS; Miltenyi Biotec). For DC isolation, spleens were digested with collagenase and enriched for DCs on a density gradient (Vremec and Shortman, 1997) followed by a two-step magnetic selection using a depletion of $B220^+$ (clone RA3.6B2) and $Gr1^+$ cells and a positive selection of $CD11c^+$ (clone N814) cells (Miltenyi Biotec). The purity of isolated T cells (>94%) and DCs (>92%) was confirmed by FACS analysis.

JCaM2 cells, PBLs, Jurkat 8.2, and naive T cells were labeled with Laurdan (6-dodecanoyl-2-dimethylaminonaphtalene; Invitrogen) by incubating cell suspensions ($0.5–2 \times 10^6$ cells/ml) in 5 μM Laurdan in RPMI with 1% FBS for 30–60 min at 37°C. APCs (DCs or CH27 B cells; $0.5–1 \times 10^7$) were incubated with 2 μM CMRA (CellTracker Orange; Invitrogen) in RPMI with 10% FBS for 15 min at 37°C followed by a further 30-min incubation at 37°C in fresh RPMI with 10% FBS. For antigen pulsing, APCs were incubated with 2 μM MCC peptide 87–103 (Queensland Institute of Medical Research) for 30–60 min at 37°C and were washed twice before conjugation.

Anti–α-CD3 mAb TR66 was obtained from A. Lanzavecchia (Institute for Research in Biomedicine, Bellinzona, Switzerland), and anti-TfR mAb and anti-CD28 antibody were purchased from BD Biosciences. Goat anti–mouse IgG polystyrene particles (3.0–3.9 μm) were obtained from Spherotech. Beads were coated with mAbs by incubating 2 μg of total antibody mixture with 10^7 beads as previously described (Harder and Kuhn, 2001).

Cell conjugation

Cells (0.5–2 × 10^6) were conjugated to coated beads (1:2 bead to cell ratio) or APCs (2:1–5:1 T cell to APC ratio) in 200 μl RPMI with 1% FBS, incubated on ice for 2–5 min, and pelleted at 800 g for 10–20 s at 4°C followed by resuspension and incubation at 37°C for indicated lengths of time. Ice-cold buffer H (800 μL of 10 mM Hepes, pH 7.2, 250 mM sucrose, and 2 mM $MgCl_2$) was added, and the cell conjugates adhered to poly-L-lysine (Sigma-Aldrich)–coated microscope coverslips, were fixed in 3.6% PFA in PBS for 20–30 min at RT, and were mounted on microscope slides (Harder and Kuhn, 2000).

Pharmacological treatments

Where indicated, cells were pretreated with 10 μM PP2 or PP3 (10-mM stock in DMSO; Calbiochem) for 1 h at 37°C before conjugation; PP2 or PP3 was also present during the conjugation and subsequent 7-min incubation at 37°C as described previously (Harder and Kuhn, 2000). Cholesterol depletion was performed with 10 mM mβCD (Sigma-Aldrich) for 20 min or 4 mM mβCD for 40 min at 37°C in RPMI with 1 mg/ml fatty acid–free BSA (Sigma-Aldrich). To determine cholesterol removal, JCaM2 cells were labeled with [^{3}H]-cholesterol as described previously (Harder and Kuhn, 2000). Cholesterol-depleted cells were washed twice with RPMI with 1% PBS before conjugation. To disrupt the actin cytoskeleton, cells were incubated with 12.5 μM latrunculin B (Calbiochem) for an additional 3 min at 37°C after conjugation and an incubation for 7 min at 37°C (Hartgroves et al., 2003).

Microscopy

All images were obtained with a microscope (model DM IRE2; Leica). Laurdan fluorescence was excited at 800 nm with a multiphoton laser system (Verdi/Mira 900; Coherent). Laurdan intensity images were recorded simultaneously with emission in the range of 400–460 nm and 470–530 nm for the two channels, respectively. The relative sensitivity of the two channels was calibrated with 5 μM Laurdan in DMSO for each experiment. Variations across imaged areas as a result of excitement with polarized light were kept to a minimum, and GP values of Laurdan in DMSO varied <2% across the imaging area. For confocal microscopy, a helium–neon laser was used to excite Cy3 or CMRA (excitation, 543 nm; emission, 550–620 nm) and Cy5 (excitation, 633 nm; emission, 650–720 nm) with appropriate cut-off filters and pinhole widths. For all images, a 100× NA 1.4 oil objective (Leica) was used and imaged at RT.

Image analysis

All image calculations were performed in floating point format, and images were converted into eight-bit unsigned images for presentation by using WiT imaging software (Coreco Imaging). The GP, defined as

$$GP = \frac{I_{(400\text{-}460)} - I_{(470\text{-}530)}}{I_{(400\text{-}460)} + I_{(470\text{-}530)}}$$

was calculated for each pixel by using the two Laurdan intensity images. GP images were pseudocolored in Adobe Photoshop. Background values (<7% of the maximum intensity) were set to zero and colored black. GP distributions were obtained from the histograms of GP images, normalized (sum = 100), and fitted to Gaussian distributions using the nonlinear fitting algorithm (Microsoft Excel). To determine GP values at the contact sites or synapses, the mean GP area of the region of interest adjacent to the bead or APC was determined as indicated in Fig. 1 A. The contact area was 0.35–0.6-μm wide and contained 7–13 (beads) or 11–18% (APC) of the imaged cell cross sections. Each data point (or symbol) in the scatter plots represents one contact site. GP values were corrected using G factor obtained for Laurdan in DMSO for each experiment (Gaus et al., 2003). 3D reconstructions were carried using VGStudio Max 1.2 software (Volume Graphics).

Statistics

Means and SDs of two populations were compared with unpaired *t* tests assuming unequal variances. For multiple comparisons, one-way analysis of variance between groups with Tukey's post-testing was performed assuming Gaussian distributions (PRISM).

We would like to thank Neil Barclay and Anton van der Merwe for their support and critical reading of the manuscript. We thank Arthur Weiss and Joseph Lin for providing the JCaM2 cells and LAT constructs.

The work in T. Harder's laboratory was supported by the Medical Research Council Cooperative Component G0100252 of the Component grant G0000764 Immune Recognition. K. Gaus was supported by the Australian Research Council, the Australian National Health and Medical Research Council, and the Australian National Heart Foundation.

Submitted: 9 May 2005
Accepted: 6 September 2005

References

Acuto, O., and F. Michel. 2003. CD28-mediated co-stimulation: a quantitative support for TCR signalling. *Nat. Rev. Immunol.* 3:939–951.

Arcaro, A., C. Gregoire, N. Boucheron, S. Stotz, E. Palmer, B. Malissen, and I.F. Luescher. 2000. Essential role of CD8 palmitoylation in CD8 coreceptor function. *J. Immunol.* 165:2068–2076.

Arcaro, A., C. Gregoire, T.R. Bakker, L. Baldi, M. Jordan, L. Goffin, N. Boucheron, F. Wurm, P.A. van der Merwe, B. Malissen, and I.F. Luescher. 2001. CD8β endows CD8 with efficient coreceptor function by coupling T cell receptor/CD3 to raft-associated CD8/p56(lck) complexes. *J. Exp. Med.* 194:1485–1495.

Bagatolli, L.A., S.A. Sanchez, T. Hazlett, and E. Gratton. 2003. Giant vesicles, Laurdan, and two-photon fluorescence microscopy: evidence of lipid lateral separation in bilayers. *Methods Enzymol.* 360:481–500.

Barda-Saad, M., A. Braiman, R. Titerence, S.C. Bunnell, V.A. Barr, and L.E. Samelson. 2005. Dynamic molecular interactions linking the T cell antigen receptor to the actin cytoskeleton. *Nat. Immunol.* 6:80–89.

Brown, D.A., and E. London. 1998. Structure and origin of ordered lipid domains in biological membranes. *J. Membr. Biol.* 164:103–114.

Brown, D.A., and E. London. 2000. Structure and function of sphingolipid- and cholesterol-rich membrane rafts. *J. Biol. Chem.* 275:17221–17224.

Bunnell, S.C., V. Kapoor, R.P. Trible, W. Zhang, and L.E. Samelson. 2001. Dynamic actin polymerization drives T cell receptor-induced spreading: a role for the signal transduction adaptor LAT. *Immunity.* 14:315–329.

Bunnell, S.C., D.I. Hong, J.R. Kardon, T. Yamazaki, C.J. McGlade, V.A. Barr, and L.E. Samelson. 2002. T cell receptor ligation induces the formation of dynamically regulated signaling assemblies. *J. Cell Biol.* 158:1263–1275.

del Pozo, M.A., N.B. Alderson, W.B. Kiosses, H.H. Chiang, R.G. Anderson, and M.A. Schwartz. 2004. Integrins regulate Rac targeting by internalization of membrane domains. *Science.* 303:839–842.

Douglass, A.D., and R.D. Vale. 2005. Single-molecule microscopy reveals plasma membrane microdomains created by protein-protein networks that exclude or trap signaling molecules in T cells. *Cell.* 121:937–950.

Dower, N.A., S.L. Stang, D.A. Bottorff, J.O. Ebinu, P. Dickie, H.L. Ostergaard, and J.C. Stone. 2000. RasGRP is essential for mouse thymocyte differentiation and TCR signaling. *Nat. Immunol.* 1:317–321.

Dykstra, M., A. Cherukuri, and S.K. Pierce. 2001. Rafts and synapses in the spatial organization of immune cell signaling receptors. *J. Leukoc. Biol.* 70:699–707.

Dykstra, M., A. Cherukuri, H.W. Sohn, S.J. Tzeng, and S.K. Pierce. 2003. Location is everything: lipid rafts and immune cell signaling. *Annu. Rev. Immunol.* 21:457–481.

Fazekas de St. Groth, B., P.A. Patten, W.Y. Ho, E.P. Rock, and M.M. Davis. 1993. An analysis of T cell receptor-ligand interaction using a transgenic antigen model for T cell tolerance and T cell receptor mutagenesis. *In* Molecular Mechanisms of Immunological Self-Recognition. F.W. Alt and H.J. Vogel, editors. Academic Press, San Diego, CA. 123–127.

Freiberg, B.A., H. Kupfer, W. Maslanik, J. Delli, J. Kappler, D.M. Zaller, and A. Kupfer. 2002. Staging and resetting T cell activation in SMACs. *Nat. Immunol.* 3:911–917.

Gaus, K., E. Gratton, E.P. Kable, A.S. Jones, I. Gelissen, L. Kritharides, and W. Jessup. 2003. Visualizing lipid structure and raft domains in living cells with two-photon microscopy. *Proc. Natl. Acad. Sci. USA.* 100:15554–15559.

Glebov, O.O., and B.J. Nichols. 2004. Lipid raft proteins have a random distribution during localized activation of the T-cell receptor. *Nat. Cell Biol.* 6:238–243.

Harder, T. 2004. Lipid raft domains and protein networks in T-cell receptor signal transduction. *Curr. Opin. Immunol.* 16:353–359.

Harder, T., and K. Simons. 1999. Clusters of glycolipid and glycosylphosphatidylinositol-anchored proteins in lymphoid cells: accumulation of actin regulated by local tyrosine phosphorylation. *Eur. J. Immunol.* 29:556–562.

Harder, T., and M. Kuhn. 2000. Selective accumulation of raft-associated membrane protein LAT in T cell receptor signaling assemblies. *J. Cell Biol.* 151:199–208.

Harder, T., and M. Kuhn. 2001. Immunoisolation of TCR signaling complexes from Jurkat T leukemic cells. *Sci. STKE.* 10.1126/stke.2001.71.pl1.

Hartgroves, L.C., J. Lin, H. Langen, T. Zech, A. Weiss, and T. Harder. 2003.

Synergistic assembly of linker for activation of T cells signaling protein complexes in T cell plasma membrane domains. *J. Biol. Chem.* 278:20389–20394.

Huppa, J.B., and M.M. Davis. 2003. T-cell-antigen recognition and the immunological synapse. *Nat. Rev. Immunol.* 3:973–983.

Janes, P.W., S.C. Ley, A.I. Magee, and P.S. Kabouridis. 2000. The role of lipid rafts in T cell antigen receptor (TCR) signalling. *Semin. Immunol.* 12:23–34.

Kabouridis, P.S., J. Janzen, A.L. Magee, and S.C. Ley. 2000. Cholesterol depletion disrupts lipid rafts and modulates the activity of multiple signaling pathways in T lymphocytes. *Eur. J. Immunol.* 30:954–963.

Katagiri, Y.U., N. Kiyokawa, and J. Fujimoto. 2001. A role for lipid rafts in immune cell signaling. *Microbiol. Immunol.* 45:1–8.

Kindzelskii, A.L., R.G. Sitrin, and H.R. Petty. 2004. Cutting edge: optical microspectrophotometry supports the existence of gel phase lipid rafts at the lamellipodium of neutrophils: apparent role in calcium signaling. *J. Immunol.* 172:4681–4685.

Krawczyk, C., and J.M. Penninger. 2001. Molecular controls of antigen receptor clustering and autoimmunity. *Trends Cell Biol.* 11:212–220.

Kusumi, A., I. Koyama-Honda, and K. Suzuki. 2004. Molecular dynamics and interactions for creation of stimulation-induced stabilized rafts from small unstable steady-state rafts. *Traffic.* 5:213–230.

Lin, J., and A. Weiss. 2001. Identification of the minimal tyrosine residues required for linker for activation of T cell function. *J. Biol. Chem.* 276: 29588–29595.

Matthias, L.J., P.T. Yam, X.M. Jiang, N. Vandegraaff, P. Li, P. Poumbourios, N. Donoghue, and P.J. Hogg. 2002. Disulfide exchange in domain 2 of CD4 is required for entry of HIV-1. *Nat. Immunol.* 3:727–732.

Monks, C.R., B.A. Freiberg, H. Kupfer, N. Sciaky, and A. Kupfer. 1998. Three-dimensional segregation of supramolecular activation clusters in T cells. *Nature.* 395:82–86.

Montixi, C., C. Langlet, A.M. Bernard, J. Thimonier, C. Dubois, M.A. Wurbel, J.P. Chauvin, M. Pierres, and H.T. He. 1998. Engagement of T cell receptor triggers its recruitment to low-density detergent-insoluble membrane domains. *EMBO J.* 17:5334–5348.

Munro, S. 2003. Lipid rafts: elusive or illusive? *Cell.* 115:377–388.

Orange, J.S., K.E. Harris, M.M. Andzelm, M.M. Valter, R.S. Geha, and J.L. Strominger. 2003. The mature activating natural killer cell immunologic synapse is formed in distinct stages. *Proc. Natl. Acad. Sci. USA.* 100:14151–14156.

Rodgers, W., D. Farris, and S. Mishra. 2005. Merging complexes: properties of membrane raft assembly during lymphocyte signaling. *Trends Immunol.* 26:97–103.

Samelson, L.E. 2002. Signal transduction mediated by the T cell antigen receptor: the role of adapter proteins. *Annu. Rev. Immunol.* 20:371–394.

Sankaram, M.B., and T.E. Thompson. 1991. Cholesterol-induced fluid-phase immiscibility in membranes. *Proc. Natl. Acad. Sci. USA.* 88:8686–8690.

Seder, R.A., W.E. Paul, M.M. Davis, and B. Fazekas de St. Groth. 1992. The presence of interleukin 4 during in vitro priming determines the lymphokine-producing potential of $CD4^+$ T cells from T cell receptor transgenic mice. *J. Exp. Med.* 176:1091–1098.

Sharma, P., R. Varma, R.C. Sarasij, K. Ira Gousset, G. Krishnamoorthy, M. Rao, and S. Mayor. 2004. Nanoscale organization of multiple GPI-anchored proteins in living cell membranes. *Cell.* 116:577–589.

Simons, K., and E. Ikonen. 1997. Functional rafts in cell membranes. *Nature.* 387:569–572.

Simons, K., and D. Toomre. 2000. Lipid rafts and signal transduction. *Nat. Rev. Mol. Cell Biol.* 1:31–39.

Tavano, R., G. Gri, B. Molon, B. Marinari, C.E. Rudd, L. Tuosto, and A. Viola. 2004. CD28 and lipid rafts coordinate recruitment of Lck to the immunological synapse of human T lymphocytes. *J. Immunol.* 173:5392–5397.

Tomlinson, M.G., J. Lin, and A. Weiss. 2000. Lymphocytes with a complex: adapter proteins in antigen receptor signaling. *Immunol. Today.* 21: 584–591.

van der Merwe, P.A. 2002. Do T cell receptors do it alone? *Nat. Immunol.* 3:1122–1123.

Varma, R., and S. Mayor. 1998. GPI-anchored proteins are organized in submicron domains at the cell surface. *Nature.* 394:798–801.

Villalba, M., K. Bi, F. Rodriguez, Y. Tanaka, S. Schoenberger, and A. Altman. 2001. Vav1/Rac-dependent actin cytoskeleton reorganization is required for lipid raft clustering in T cells. *J. Cell Biol.* 155:331–338.

Villalba, M., K. Bi, J. Hu, Y. Altman, P. Bushway, E. Reits, J. Neefjes, G. Baier, R.T. Abraham, and A. Altman. 2002. Translocation of PKC[τ] in T cells is mediated by a nonconventional, PI3-K- and Vav-dependent pathway, but does not absolutely require phospholipase C. *J. Cell Biol.* 157:253–263.

Viola, A., S. Schroeder, Y. Sakakibara, and A. Lanzavecchia. 1999. T lymphocyte costimulation mediated by reorganization of membrane microdomains. *Science.* 283:680–682.

Vremec, D., and K. Shortman. 1997. Dendritic cell subtypes in mouse lymphoid organs. Cross-correlation of surface markers, changes with incubation and differences among thymus, spleen and lymph nodes. *J. Immunol.* 159:565–573.

Wilde, J.I., and S.P. Watson. 2001. Regulation of phospholipase C gamma isoforms in haematopoietic cells: why one, not the other? *Cell. Signal.* 13:691–701.

Zacharias, D.A., J.D. Violin, A.C. Newton, and R.Y. Tsien. 2002. Partitioning of lipid-modified monomeric GFPs into membrane microdomains of live cells. *Science.* 296:913–916.

Zhang, W., J. Sloan-Lancaster, J. Kitchen, R.P. Trible, and L.E. Samelson. 1998a. LAT: the ZAP-70 tyrosine kinase substrate that links T cell receptor to cellular activation. *Cell.* 92:83–92.

Zhang, W., R.P. Trible, and L.E. Samelson. 1998b. LAT palmitoylation: its essential role in membrane microdomain targeting and tyrosine phosphorylation during T cell activation. *Immunity.* 9:239–246.